Structural Eng./Earthquake Eng., JSCE, Vol. 16, No. 2, 111s—124s, 1999 October
(J. Struct. Mech. Earthquake Eng., JSCE, No. 633/ I —49)

COMPARATIVE STUDY OF FOUR HYSTERETIC MODELS FOR PIPE-SECTION STEEL BRIDGE PIERS

Qingyun LIU[1], Akira KASAI[2] and Tsutomu USAMI[3]

[1] Student Member of JSCE, M. of Eng., Graduate Student, Dept. of Civil Eng., Nagoya University
(Furocho, Chikusa-ku, Nagoya 464-8603, Japan)
[2] Member of JSCE, M. of Eng., Research Associate, Dept. of Civil Eng., Nagoya University
(Furocho, Chikusa-ku, Nagoya 464-8603, Japan)
[3] Fellow of JSCE, Dr. of Eng., Dr. of Sc., Professor, Dept. of Civil Eng., Nagoya University
(Furocho, Chikusa-ku, Nagoya 464-8603, Japan)

This paper presents inter-comparison among four hysteretic models for inelastic seismic response analysis of cantilever-type steel bridge piers: the bilinear model, the trilinear model, the integrated 2 parameter model and the damage-based hysteretic model. It is shown that the commonly used bilinear model is not suitable to predict residual displacement in analysis. The trilinear model is a better choice than the bilinear model, but cautions should be taken in its application due to its non-degrading, kinematic hardening formulation. Except for residual displacement under Level 2 · Type I · Ground Type III accelerograms, very good agreement is found between the damage-based hysteretic model and the integrated 2 parameter model within the range of $H_r \geq H_y$ (H_r is the predicted horizontal strength).

Key Words: hysteretic model, seismic analysis, steel bridge piers, residual displacement

1. INTRODUCTION

According to the current Design Specifications of Highway Bridges of Japan Road Association[1] (the JRA code), state-of-practice in the seismic design of steel bridge piers follows a two-phase procedure—serviceability design and ultimate limit state design. Seismic coefficient method is prescribed in the JRA code for serviceability design, which is to ensure elastic behavior (no damage) during moderate (and highly probable) earthquakes. For check of ultimate limit state, however, the JRA code falls short of providing an appropriate ductility design method for hollow steel bridge piers (without concrete filling) due to inadequate understanding of the inelastic earthquake resisting mechanism of these structures. Instead, the JRA code recommends dynamic analysis be carried out to safeguard against collapse in case of a severe earthquake.

Inelastic seismic response analysis of cantilever-type steel bridge piers suggested by the JRA code for ultimate limit state design of these structures requires quick and reliable prediction of hysteretic behavior, and many hysteretic models based on different concepts have been proposed for this purpose. The most representative hysteretic models found in literature for dynamic analysis of hollow steel bridge piers of cantilever type are: the bilinear model, the trilinear model, 2 parameter model[2] (this study makes use of its modified version—the integrated 2 parameter model) and the damage-based hysteretic model[3)-5]. These models range from simple but unrealistic (the bilinear model) to complicated but more realistic (the damage-based hysteretic model). This paper aims to gain some insights into practical performance of these models through inter-comparison among these models. Following this introduction, major features of each model are first explained and innate limit of application due to assumptions and concepts behind the formulation of each model is emphasized. Presented secondly is simulation of pseudodynamic tests by all these models. Next, performances of the four models are compared under design conditions. Recommendations for their application are made in conclusion. For simplicity, discussion heretofore is limited to pipe-section steel bridge piers, but findings obtained in this study may readily apply to box-section steel bridge piers.

2. HYSTERETIC MODELS

(1) Bilinear model

The most simple and commonly used hysteretic model is the bilinear model. The main features of

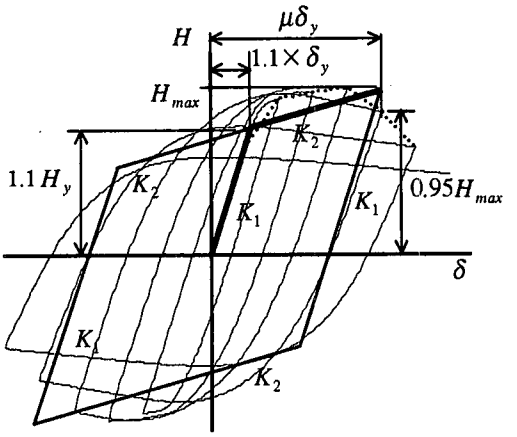

Fig.1 Definition of bilinear model

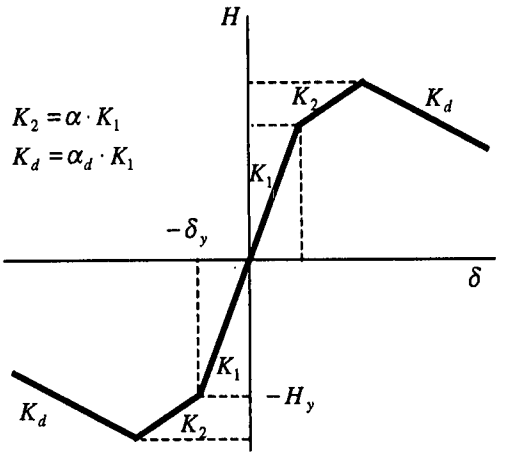

Fig.2 Primary curve of trilinear model

the bilinear model can be summarized as: non-degrading (neither stiffness nor strength deteriorates with inelastic deformation) and kinematic hardening (nominal elastic range remains constant). Hysteretic loops from this model always take the shape of a parallelogram (**Fig.1**), and the model can fully be defined by a bilinear primary curve. Definition of the bilinear model in this study follows partly the example found in the JRA code[1)] and is illustrated in **Fig.1**. Note that intersection of the two limbs of the primary curve is set at $(1.1\delta_y,\ 1.1H_y)$, wherein δ_y is the yield displacement of the bridge pier, and H_y the yield load. $\mu\delta_y$ in **Fig.1** also defines the suitable application range of bilinear model — because of its non-degrading nature, application of the model obviously should be confined by the actual cyclic hardening range (μ is allowable ductility ratio). Here, $\mu\delta_y$ is designated as the displacement value that corresponds to the cyclic strength dropping to $0.95H_{max}$ — δ_{95}, wherein H_{max} is the maximum strength that can be reached under cyclic loading. In this study, empirical equations for δ_{95} and H_{max} given in Ref.6 are used in defining bilinear model:

$$\mu=\frac{\delta_{95}}{\delta_y}=\frac{0.24}{(1+P/P_y)^{2/3}R_t\bar{\lambda}^{1/3}} \tag{1}$$

$$\frac{H_{max}}{H_y}=\frac{0.02}{(R_t\bar{\lambda})^{0.8}}+1.10 \tag{2}$$

where P/P_y is axial load ratio; R_t is radius thickness ratio parameter and $\bar{\lambda}$ slenderness ratio parameter. R_t and $\bar{\lambda}$ for pipe-section steel bridge piers are defined as[1)]:

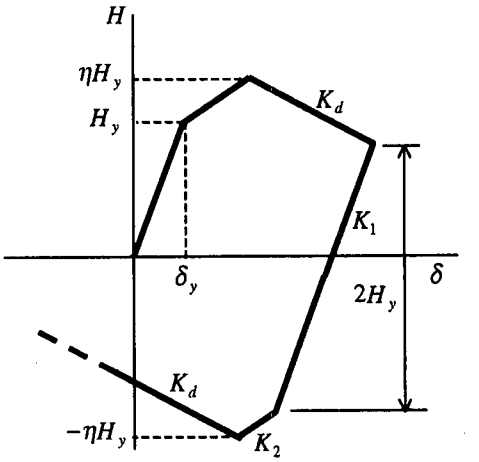

Fig.3 Hysteretic rules of trilinear model

$$R_t=\sqrt{3(1-\nu^2)}\frac{\sigma_y}{E}\frac{D}{2t} \tag{3}$$

$$\bar{\lambda}=\frac{2h}{r}\frac{1}{\pi}\sqrt{\frac{\sigma_y}{E}} \tag{4}$$

wherein σ_y is yield stress of steel; E is Young's modulus; ν is Poisson's ratio; D and t are diameter and thickness of the cross section respectively; h is column height and r denotes radius of gyration of the cross section.

(2) Trilinear model

Formulation of the trilinear model is very similar to that of the bilinear model except that the primary curve consists of three limbs— an elastic limb, a hardening plastic limb and a descending plastic limb (**Fig.2**). It is also a non-degrading, and kinematic hardening model, and its hysteretic rules are illustrated in **Fig.3**. The overall nominal elastic

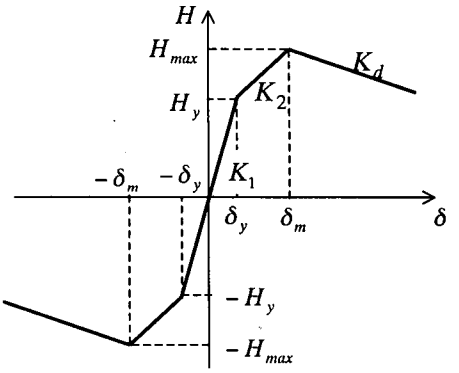

Fig.4 Skeleton curve of 2-para model

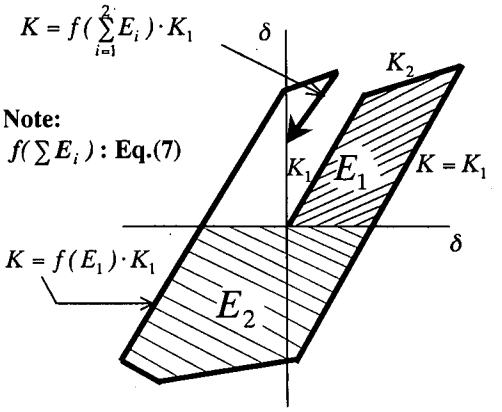

Fig.5 Determination of current stiffness K (2-para model)

range remains as $2H_y$, and the maximum strength on either side keeps constant at ηH_y. Besides, the unloading stiffness always equals the initial elastic stiffness K_1. It is obvious that trilinear model is fully defined by three parameters[7]: α (stiffness ratio of the hardening limb to the elastic limb), α_d (stiffness ratio of the softening limb to the elastic limb), and peak strength ratio η. In this study, peak strength ηH_y is designated as H_{max} by Eq.(2); α is fixed at 0.4, and α_d at -0.08 through trial-and-error following the practice of Ref.7.

Obviously, neither the bilinear model nor the trilinear model can realistically simulate cyclic behavior of thin-walled steel bridge piers (See Appendix C), which is characterized by high rate of strength and stiffness degradation. However, they are still widely used in seismic response analysis because of simplicity.

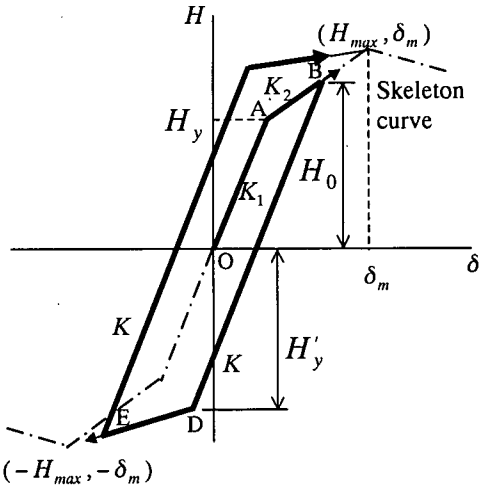

Fig.6 Hysteretic rules of the hardening stage (2-para model)

(3) Integrated 2 parameter model (2-para model)

The original 2 parameter model[2] was proposed based on cyclic test of box-section steel bridge piers, and it actually consisted of three sub-models with different hysteretic rules, named Type "A", Type "B" and Type "C" (major differences among the three sub-models are summarized in **Appendix A**). Each type applies to a group of bridge piers whose structural parameters fall within a specified range, and the three combined to cover the entire range of structural parameters of practical interest. In adapting 2 parameter model for use with pipe-section steel bridge piers, it is recognized that by varying model parameters continuously with structural parameters, an integrated model may as well cover the whole possible range of structural parameters without type classification. In what follows, the integrated 2 parameter model (heretofore referred to as 2-para model) for pipe-section steel bridge piers is presented, and features different from the original 2 parameter model are highlighted.

a) Skeleton curve

Definition of the skeleton curve in 2-para model completely follows that of the original 2 parameter model and **Fig.4** shows the trilinear skeleton curve. In addition to H_y and δ_y, which can be calculated analytically, three other quantities are needed to fully determine this curve: H_{max}, δ_m and K_d. The point (H_{max}, δ_m) defines the peak loading point that can be reached under cyclic loading; As mentioned in definition of bilinear model, H_{max} can be calculated with Eq.(2) and Ref.6 also gives

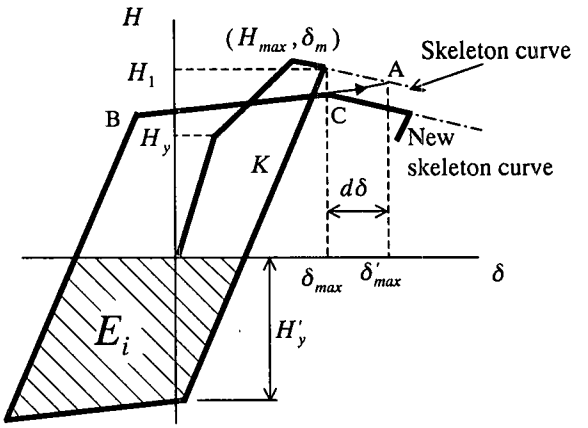

Fig.7 Hysteretic rules of the degrading stage (2-para model)

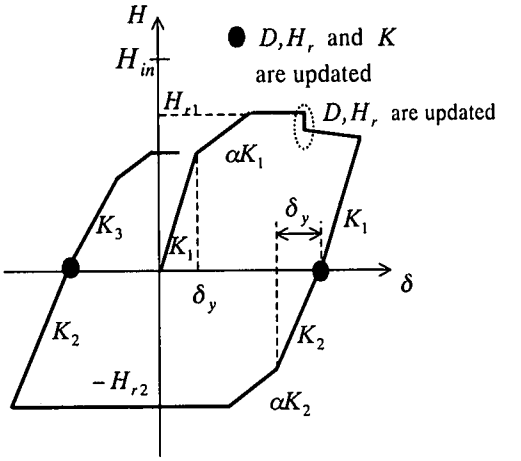

Fig.8 Image of D model

the empirical equation of δ_m for pipe-section steel bridge piers:

$$\frac{\delta_m}{\delta_y} = \frac{1}{3\left(R_t \bar{\lambda}^{0.5}\right)^{0.8}} - \frac{2}{3} \tag{5}$$

Stiffness of the descending branch, K_d, is supposed to be equal to that of monotonic horizontal load—displacement curve, and based on monotonic FEM analysis results, it can be approximated by:

$$\frac{K_d}{K_1} = -1.41 R_t \left(1 + \frac{P}{P_y}\right)^5 \bar{\lambda}^{1.3} \tag{6}$$

wherein $K_1 = H_y / \delta_y$ is the initial elastic stiffness.

b) Hysteretic rules

The 2-para model takes into account the following observed cyclic behaviors through its hysteretic rules: 1) cyclic hardening effect; 2) stiffness degradation; 3) strength degradation. The loading history is divided into two stages in the modeling: the hardening stage and the degrading stage. The hardening stage is the initial loading stage while the displacement stays within $\pm\delta_m$, and behavior of the structure is characterized by cyclic hardening effect; the degrading stage begins once the displacement moves out of the range of $\pm\delta_m$, and the hysteretic behavior is marked by deterioration of strength. The above division of hardening stage and degrading stage comes as a major modification to the original 2 parameter model. Originally, this division is separately defined on the positive side and the negative side, that is, $+\delta_m$ serves as the threshold of the positive side and $-\delta_m$ the threshold on the negative side. Thus initiation of degrading behavior on one side has nothing to do with the behavior on the other side. It is found that such severed treatment leads to unrealistic modeling: a case in point is when a specimen undergoes one-sided cyclic loading. Cyclic test results as well as FEM analysis results unequivocally show that behaviors on the two sides are related; strength on the opposite side actually will deteriorate with the positive displacement cycling even if the displacement can never reach $-\delta_m$. Interested readers are referred to **Appendix B** for an illustration of effect of this modification.

Consideration of stiffness degradation follows strictly the idea of the original model (**Fig.5**). It is considered throughout the two stages whenever unloading occurs; unloading stiffness K is related to accumulated hysteretic energy $\sum E_i$ by:

$$\frac{K}{K_1} = 1 - \frac{1}{\alpha} ln\left(\frac{\sum E_i / E_e}{100} + 1\right) \tag{7}$$

The empirical parameter $\bar{\alpha}$ in Eq.(7) is determined from extensive FEM analysis results of pipe-section steel bridge piers as follows:

$$\bar{\alpha} = \frac{1}{7.36 R_t} \tag{8}$$

Note that $E_e = H_y \delta_y / 2$ is used to normalize the accumulated hysteretic energy $\sum E_i$ in Eq.(7).

Fig.6 illustrates the hysteretic rules of 2-para model during the initial hardening stage. Starting from point O, the initial yield occurs at point A; beyond point A, the loading point follows a plastic hardening limb heading toward peak point of the skeleton curve (H_{max}, δ_m); suppose before reaching the peak point, there is unloading from point B at a strength level of H_0; cyclic hardening is modeled by stretching the 'elastic' limb beyond the initial yield load H_y when reloading, and the elastic

range is now updated to:

$$H_y' = H_y + \gamma(H_0 - H_y) \quad (9)$$

wherein γ =hardening factor calculated by

$$\gamma = 1.2 - 10R_t \qquad (0 \le \gamma \le 1) \quad (10)$$

Beyond the hardened elastic range on the opposite side, the loading point is directed toward peak point of the skeleton curve on the opposite side ($-H_{max}$, $-\delta_m$) (D to E in **Fig.6**); if at unloading from point E, the displacement still falls within hardening stage, the 'elastic' limb will be stretched again, and so on.

In the original model, cyclic hardening effect is considered only in sub-model Type "B" by equating H_y' to H_0. Through the hardening factor γ, the new 2-para model comes to consider cyclic hardening for different bridge piers to a different extent. Obviously, this modification not only enables simplification of the hysteretic model itself but also offers more reasonable modeling of the actual structural behavior.

Now referring to **Fig.7** for an explanation of the hysteretic rules during the degrading stage. Strength degradation is modeled by the following treatments: Firstly, the elastic range starts to shrink, which is expressed by:

$$\begin{aligned} H_y' &= K\delta_y + \gamma(H_1 - H_y) \quad (\text{if } H_1 > H_y) \\ H_y' &= K\delta_y \qquad\qquad\qquad (\text{if } H_1 \le H_y) \end{aligned} \quad (11)$$

wherein H_1 is the strength at the unloading point in **Fig.7**, and K the current stiffness given by Eq.(7). It is obvious that Eq.(11) expresses shrinking of elastic range in terms of strength and stiffness deterioration. Secondly, the loading point is directed toward an image point on the descending branch of the skeleton curve after yielding, thus forming a plastic hardening limb (BC in **Fig.7**). The image point (point A in **Fig.7**) is designated by: $\delta_{max}' = \delta_{max} + d\delta$, and $d\delta = \bar{\beta} \cdot E_i / H_{max}$, wherein $\bar{\beta}$ is the strength degradation factor. It is obvious that a larger $\bar{\beta}$ shall result in faster strength degradation. Through careful calibration, parameter $\bar{\beta}$ is given as:

$$\bar{\beta} = \frac{1}{3}(5R_t + 0.25) \quad (12)$$

Next, motion of the loading point follows a literally descending branch with the stiffness of K_d if the loading point tends to move beyond the current maximum displacement δ_{max} (motion of the loading point after point C in **Fig.7**). And finally, the latest formed descending branch shall serve as new skeleton curve in determining the image point for further loading cycles on the same side.

The hysteretic rules of 2-para model during the degrading stage are adapted from those of the original model (sub-model Type "A"). Modifications have been made on two points: one is about calculation of elastic range; the other is about parameter $\bar{\beta}$. Originally, the shrinking of elastic range is ruled as $H_y' = H_1 \cdot H_y / H_{max}$ which gives the value of H_y' always below H_y. Since 2-para model has newly incorporated cyclic hardening effect which the original sub-model Type "A" did not account for during the initial hardening stage, the elastic range (starting from H_y) is expected to continuously expand until the displacement moves out of $\pm\delta_m$ and sets off degrading behavior. Using the original rule would result in a sudden contract of the elastic range at the beginning of the degrading stage, which is contrary to the actual hysteretic behavior of the structure. It is clear that Eq.(11) shall offer a much smoother transition in this regard. In the original 2 parameter model, parameter $\bar{\beta}$ was actually a type-based constant with type classification in place. The integrated 2-para model takes full advantage of this parameter in adjusting the rate of strength degradation, and makes it a function of the structural parameter R_t. This is another practice of varying model parameter continuously with structural characteristics in the stead of varying hysteretic rules. The reason for choosing original sub-model Type "A" over sub-model Type "B" and Type "C" in adaptation is that the frame of sub-model A allows the most flexibility in determining parameter $\bar{\beta}$. Ref.2 gives the full details of the original 2 parameter model and major differences among the three sub-models are summarized in **Appendix A**.

A note on parameter determination of 2-para model: parameter K_d and $\bar{\alpha}$ are summarized from extensive monotonic and cyclic FEM analysis results of pipe-section steel bridge piers with a wide range of structure parameters; parameter γ and $\bar{\beta}$ are calibrated against the same cyclic FEM analysis results. The whole procedure of the FEM analysis used is the same as that of Ref.6 .

(4) Damage-based hysteretic model[5] (D model)

The structural characteristics of thin-walled steel bridge piers make them susceptible to damage in the form of local buckling and overall interaction instability. From this point of view, deterioration of strength and stiffness under a seismic event is due to accumulation of damage in the structure. At the center of the damage-based hysteretic model is a

comprehensive damage index to quantify the seismic damage throughout the loading history. At the initial undamaged state, the damage index $D=0$; it increases with the onset of inelastic deformation and comes to unity at the assumed collapse point. Collapse is defined as the residual strength dropping to yield load H_y.

The hysteretic model is of piecewise multi-linear type. The primary curve is a trilinear curve made of an elastic limb, a hardening limb and a perfectly plastic limb. With updating of the damage index and residual strength, there may also be a descending limb in addition to the above three limbs. **Fig.8** is a schematic image of the damage-based hysteretic model. Degradation of strength and stiffness is related to damage progression by Eqs.(13)-(14):

$$H_r = H_{in} \cdot (\frac{H_y}{H_{in}})^D \quad (13)$$

$$K = K_1 \cdot (\frac{H_y}{H_{in}})^D \quad (14)$$

where K_1 is the initial elastic stiffness; H_{in} is the imaginary strength at $D=0$. Details of the damage index formulation and the accompanying hysteretic model for box-section and for pipe-section steel bridge piers can be found in Ref.3-4 and Ref.5 respectively. What is worth pointing out here is that Eqs.(13)-(14) are calibrated between $D=0$ and the collapse point $D=1$ in building the hysteretic model, thus application of the model is better limited to this range for reliable analysis results. Another distinctive feature of this model is that it does not account for cyclic hardening effect, as can be inferred from Eq.(13). Horizontal loading carrying capacity is modeled as monotonically decreasing with cyclic loading, since damage index is a function monotonically increasing with cyclic loading.

3. SIMULATION OF PSEUDODYNAMIC TESTS

Employing the above four hysteretic models to predict restoring force, time-history analysis is carried out to simulate pseudodynamic tests on pipe-section steel bridge piers[7]. The single bridge piers of cantilever type are modeled as SDOF system in the inelastic seismic response analysis. Input earthquake excitations are two accelerograms of Hyogoken-Nanbu earthquake: one was recorded by Japan Meteorological Agency (JMA) (NS component , ground type I (stiff)) and the other was observed at Higashi Kobe Bridge (HKB) (TR component, ground type III (soft)). The linear acceleration method (time interval: $\Delta t = 0.02$ sec with JMA and $\Delta t = 0.01$ sec with HKB; these time intervals are regarded as appropriate since analysis results hereby obtained bear no detectable difference from those obtained under $\Delta t = 0.001$ sec.) is used to solve the equation of motion. Damping ratio is assumed as 0.05 . Structural parameters of the analyzed specimens are listed in **Table 1**. As an illustration of simulating the pseudodynamic tests, simulated response histories and hysteretic loops of specimen TS08-30-18(JMA) are laid out in **Fig.9**. The predicted displacement responses are compared with test results in **Table 2**.

From **Table 2**, it is clear that good agreement in maximum displacement and occasional discrepancies in residual displacement are common to the performance of these hysteretic models. Test result shows that residual displacement response of TS11-30-16 to JMA is close to zero; on the other hand, all four models agree in predicting a larger response, but the absolute discrepancy is merely about $0.5\delta_y$. Looking at residual displacement response of TS11-30-11 to 1.5×HKB, D model, 2-para and trilinear model give predictions quite close to test results of about $3.0\delta_y$, while bilinear model gives a value below δ_y. There may be an explanation: the calculated allowable ductility ratio of TS11-30-11(1.5×HKB) (Eq.(1)) is 2.75; thus it can be seen that under the scaled-up HKB accelerogram, the actual structural response has exceeded the suitable application range of the bilinear model.

Generally speaking, D model, 2-para, and the trilinear model all seem to simulate adequately the pseudodynamic test results and the bilinear model tends to predict a low level of residual displacement. It should be noted, however, the above test results are too limited to give definite trends in performance of each model. Besides, the input motions are of relatively short duration and induce relatively low level of inelastic displacement (for $|\delta_{max}| < 5\delta_y$).

4. PERFORMANCE UNDER DESIGN CONDITIONS

In this section, effect of different hysteretic models on seismic analysis results is examined under design conditions. Analysis is carried out on three series of pipe-section steel bridge piers (intended for Ground Type I, II, and III respectively) designed based on seismic coefficient method. Structural parameters of the analyzed piers

Table 1 Structural parameters of pseudodynamic test specimens

Specimen (Accelerogram)	R_t	$\bar{\lambda}$	P/P_y	Mass $(kN\cdot s^2/mm)$	T (sec)	H_y (kN)	δ_y (mm)
TS11-30-16 (JMA)	0.102	0.316	0.155	1.84	0.90	5.34×10^3	59.4
TS11-30-11 (HKB)	0.119	0.338	0.111	1.48	0.81	6.27×10^3	71.1
TS11-30-11 (1.5×HKB)	0.117	0.337	0.111	1.49	0.81	6.31×10^3	70.7
TS08-30-18 (JMA)	0.081	0.318	0.181	2.75	0.98	6.59×10^3	58.0

Note: Mass, H_y, δ_y and the natural period T have been converted to those of the assumed real bridge piers (scale factor=8.0).

Table 2 Comparison of test and analysis results by different hysteretic models

Specimen (Accelerogram)	$\lvert\delta_{max}\rvert/\delta_y$					δ_R/δ_y				
	Exp.	D model	2-para	Trilinear	Bilinear	Exp.	D model	2-para	Trilinear	Bilinear
TS11-30-16 (JMA)	2.96	2.98 (1.01)	2.96 (1.00)	3.02 (1.02)	3.04 (1.03)	-0.14	-0.674 (4.79)	-0.81 (5.79)	-0.64 (4.57)	-0.49 (3.50)
TS11-30-11 (HKB)	2.47	2.69 (1.09)	2.44 (0.99)	2.47 (1.00)	2.36 (0.96)	-0.82	-1.21 (1.48)	-0.83 (1.01)	-0.77 (0.94)	-0.81 (0.99)
TS11-30-11 (1.5×HKB)	4.69	4.38 (0.93)	5.19 (1.11)	5.48 (1.17)	4.07 (0.87)	-3.10	-2.74 (0.88)	-3.36 (1.08)	-3.62 (1.67)	-0.88 (0.28)
TS08-30-18 (JMA)	3.39	3.42 (1.01)	3.05 (0.90)	3.44 (1.01)	3.11 (0.92)	-0.85	-1.25 (1.47)	-0.59 (0.69)	-1.45 (1.71)	-0.44 (0.52)
Average		(1.01)	(1.00)	(1.05)	(0.95)		(2.16)	(2.14)	(2.22)	(1.52)

Note: Values in parentheses are ratios of analysis results to test results

Table 3 Structural parameters of analyzed bridge piers

Bridge Pier	R_t	$\bar{\lambda}$	P/P_y	Ground Type	Mass $(kN\cdot s^2/mm)$	T (sec)	H_y (kN)	δ_y (mm)
AS08-20-G1	0.08	0.20	0.268	I	1.38	0.533	2.70×10^3	14.1
AS08-25-G1	0.08	0.25	0.224	I	1.17	0.686	2.29×10^3	23.4
AS08-30-G1	0.08	0.30	0.191	I	1.02	0.841	1.99×10^3	35.1
AS08-35-G1	0.08	0.35	0.166	I	0.898	0.996	1.76×10^3	49.3
AS08-40-G1	0.08	0.40	0.151	I	0.835	1.173	1.57×10^3	65.4
AS08-45-G1	0.08	0.45	0.150	I	0.837	1.402	1.40×10^3	83.0
AS08-50-G1	0.08	0.50	0.148	I	0.839	1.644	1.26×10^3	102.6
AS08-20-G2	0.08	0.20	0.225	II	1.17	0.491	2.86×10^3	14.9
AS08-25-G2	0.08	0.25	0.186	II	0.981	0.629	2.40×10^3	24.5
AS08-30-G2	0.08	0.30	0.158	II	0.847	0.767	2.07×10^3	36.6
AS08-35-G2	0.08	0.35	0.135	II	0.745	0.907	1.83×10^3	51.1
AS08-40-G2	0.08	0.40	0.117	II	0.665	1.047	1.63×10^3	68.1
AS08-45-G2	0.08	0.45	0.103	II	0.601	1.188	1.47×10^3	87.6
AS08-50-G2	0.08	0.50	0.092	II	0.559	1.341	1.34×10^3	109.4
AS08-20-G3	0.08	0.20	0.194	III	1.01	0.457	2.98×10^3	15.5
AS08-25-G3	0.08	0.25	0.159	III	0.845	0.583	2.48×10^3	25.3
AS08-30-G3	0.08	0.30	0.133	III	0.726	0.711	2.13×10^3	37.6
AS08-35-G3	0.08	0.35	0.114	III	0.636	0.838	1.87×10^3	52.3
AS08-40-G3	0.08	0.40	0.098	III	0.567	0.967	1.67×10^3	69.6
AS08-45-G3	0.08	0.45	0.085	III	0.511	1.095	1502.53	89.3
AS08-50-G3	0.08	0.50	0.074	III	0.465	1.224	1368.54	111.6

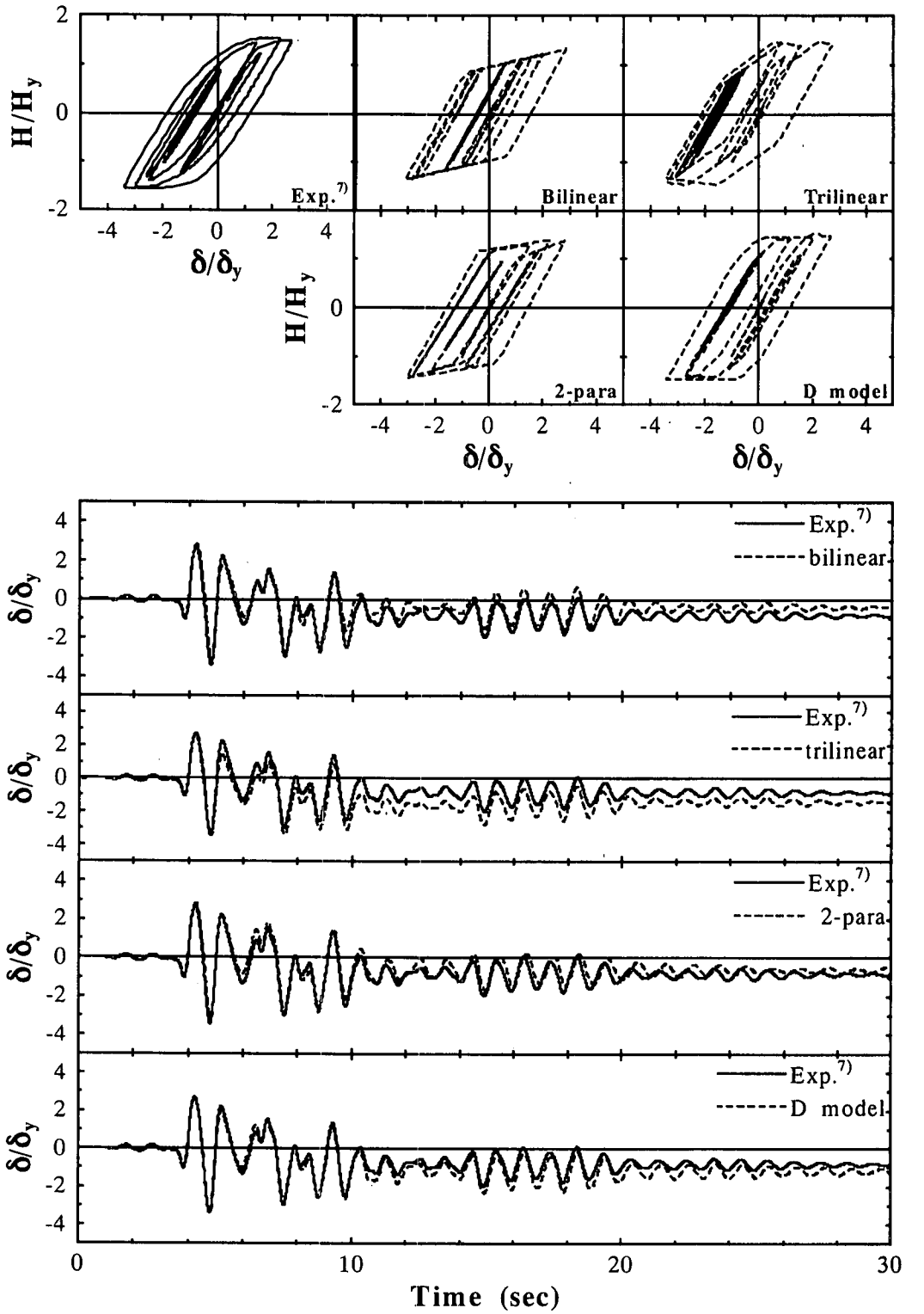

Fig.9 Simulation of Pseudodynamic test (TS08-30-18(JMA))

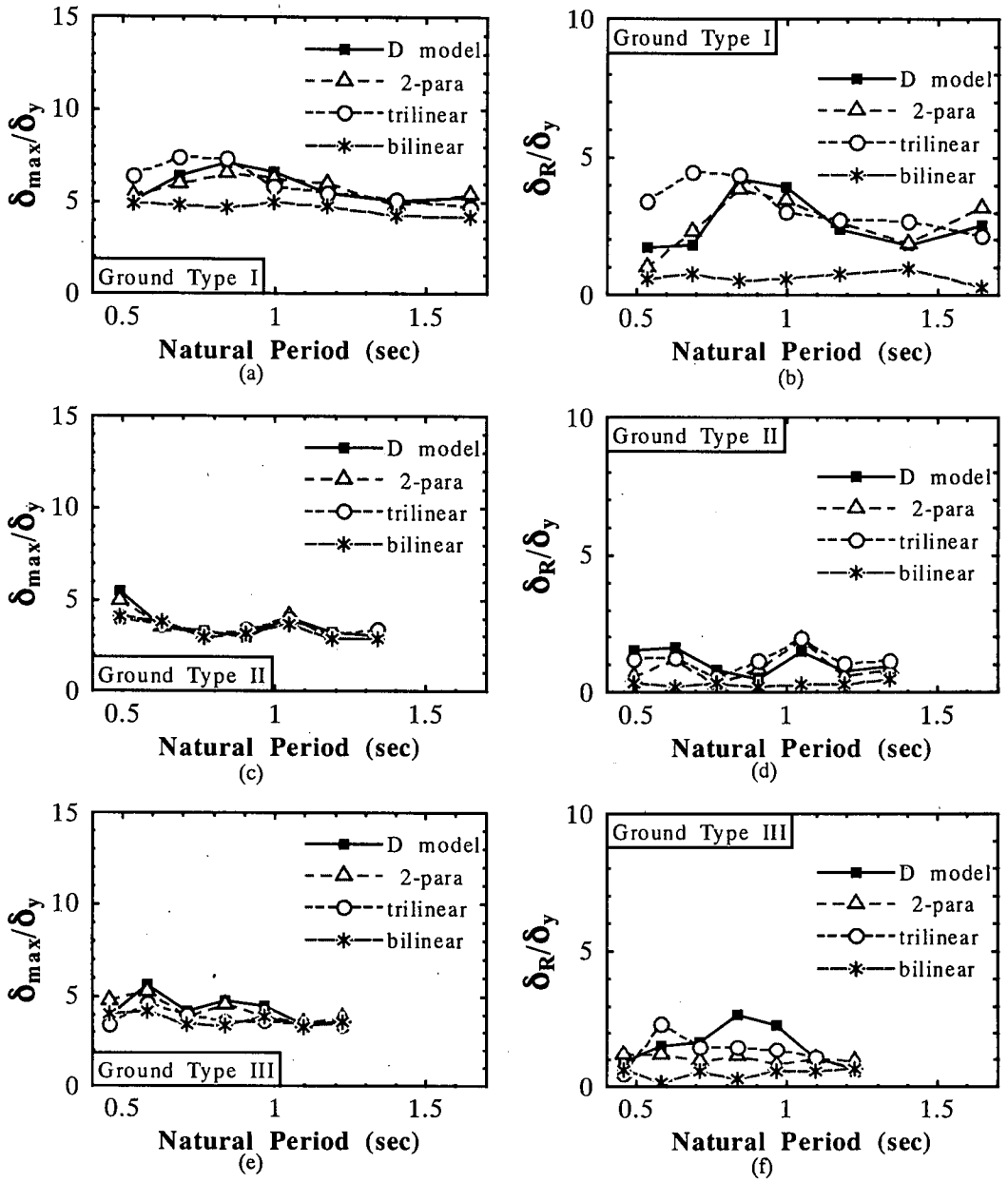

Fig. 10 Responses to Level 2 · Type I accelerograms

are listed in **Table 3**. A uniform R_t=0.08 is adopted in satisfying earthquake resistant detailing prescribed in the JRA code[1]. The code requires dynamic analysis be carried out to check response under two types of Level 2 accelerograms (Type I: plate-boundary type earthquake; Type II: inland-strike type earthquake), and suggests the average response values to all three accelerograms of the relevant ground type be taken as the final analysis results. Using the natural period as the abscissa, reponses to type I and type II accelerograms are plotted in **Fig.10** and **Fig.11** respectively.

Under all the Level 2 accelerograms, bilinear model always tends to give the lowest maximum displacement response among the four hysteretic models. A check of maximum responses against calculated allowable ductility ratio of each analyzed bridge pier turns out that maximum responses to all Type I · Ground type I accelegroms and almost all Type II accelerograms have exceeded the calculated

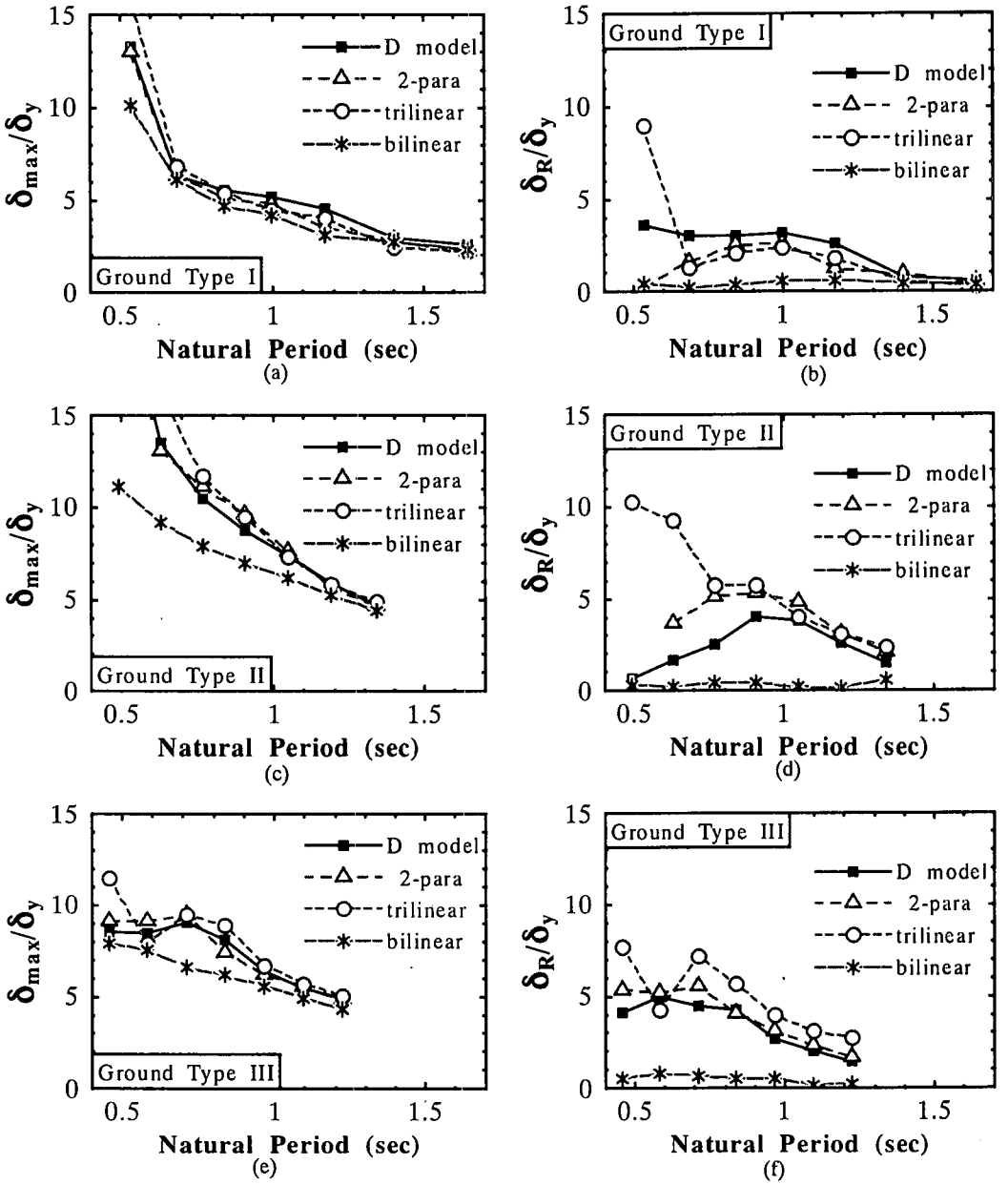

Fig. 11 Responses to Level 2 · Type II accelerograms

allowable ductility ratios. Moreover, residual displacements predicted by bilinear model are close to zero irrespective of natural periods or different accelerograms. This cast serious doubt on the reliability of this popular model in predicting residual displacement even within the allowable ductility ratio.

Referring to **Fig.10(a) (c) (e)**, under all Type I accelerograms (characterized by long duration and large number of cycles), maximum displacement predicted by D model, 2-para and trilinear model come pretty close to each other, and there is only small fluctuation in maximum displacement with variation of natural period. Looking at **Fig.10(b) (d) (f)**, the following can be said about performance of D model, 2-para model and trilinear model in predicting residual displacement under Level 2 · Type I accelerograms: (1) The agreement between D model and 2-para model under Ground Type I and Ground Type II ground motions is quite

satisfactory; (2) Under Ground Type I and Ground Type II accelerograms, the trilinear model generally have good agreement with D model and 2-para model in predicting residual displacement except for certain range of relatively short natural period (as in **Fig.10(b)**, the trilinear model the trilinear model gives much higher residual displacement level than the other two when $T \le 0.841sec$); (3) However, there seem to be little common ground among the three models in predicting residual displacement under Ground Type III accelerograms, which may be attributed to the extremely long duration of the accelerograms.

Referring to **Fig.11 (a) (c) (e)**, there is a strong trend for the maximum displacement under all Type II accelerograms (characterized by high intensity but short duration) to become larger when the natural period becomes shorter. Extremely large maximum displacement is predicted by D model, 2-para and trilinear model with the natural period below 1.0 second (2-para model fails to give final analysis results to AS08-20-G2 with a natural period of 0.491 sec because the extremely large displacement makes the calculated elastic range shrink to zero). A check of the damage index calculated by D model reveals that the damage index comes near or over collapse level (D=1.0) for those bridge piers of shorter natural period. The following can be said about performance of D model, 2-para model and the trilinear model under Level 2 · Type II accelerograms: (1)Within longer natural period range, pretty good agreement is found between D model and 2-para model in predicting both the maximum displacement and residual displacement. (2) Within the same longer period range, the trilinear model generally has good agreement with the other two except that it gives relatively higher residual displacement than the two under Ground Type III accelerograms.

5. CONCLUSIONS

In the previous sections, concepts of four different hysteretic models for seismic analysis of pipe-section steel bridge piers: bilinear model, trilinear model, the integrated 2-parameter model (2-para model) and the damage-based hysteretic mode (D model) are explained. The integrated 2-parameter model for pipe-section steel bridge piers is newly developed based on the original 2-parameter model[2] for box-section steel bridge piers. Performances of these models are compared in the context of simulating pseudodynamic tests as well as under practical design conditions.

The following conclusions can be drawn from the intercomparison among the four hysteretic models:

(1) The non-degrading kinematic hardening bilinear model can predict maximum displacement satisfactorily when used within the allowable ductility ratio, but it can't be relied upon to give reasonable residual displacement response.

(2) Although the formulation of the trilinear model is also characterized by non-degrading and kinematic hardening (as the bilinear model),

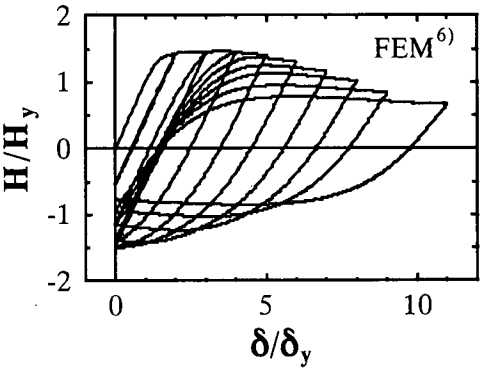

Fig.A1 Hysteretic loop under one-sided cyclic loading (FEM analysis)

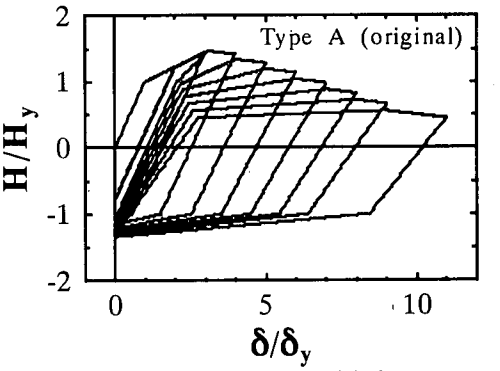

Fig.A2 Modeling by the original 2 parameter model (Type "A")

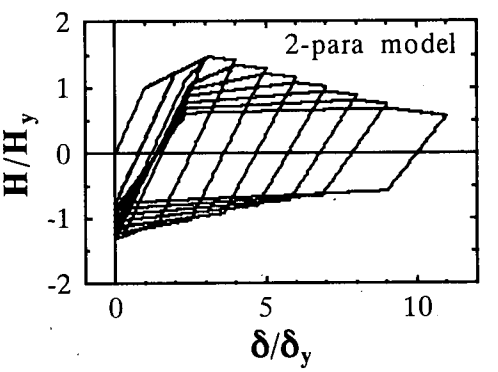

Fig.A3 Modeling by 2-para model

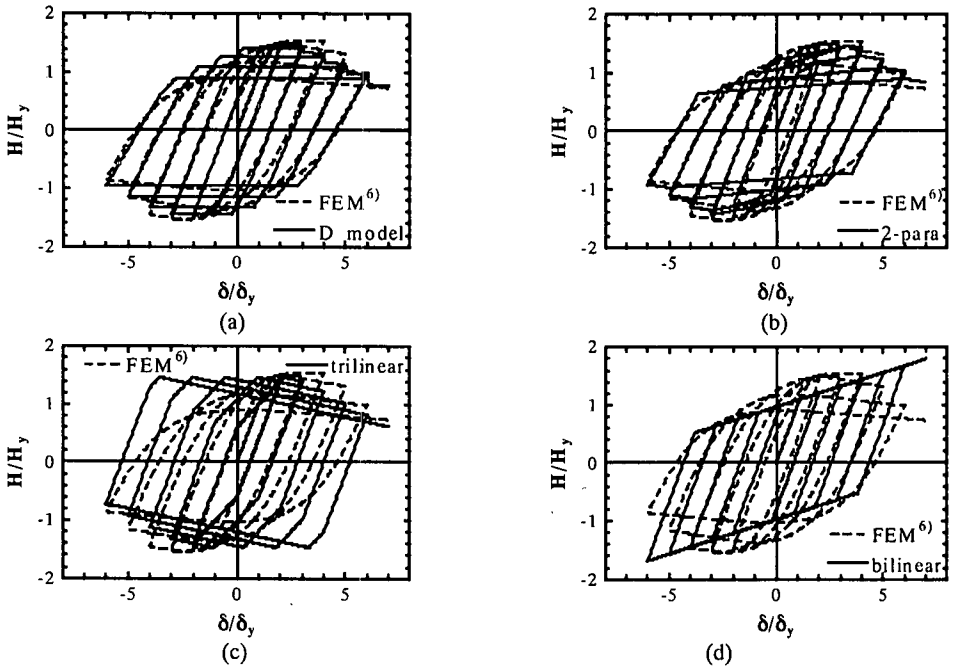

Fig.A4 Simulation of cyclic behavior ($R_t = 0.075$, $\bar{\lambda} = 0.35$, $P/P_y = 0.15$)

employing the trilinear primary curve and adding a descending limb make it a much superior model over the bilinear model. However, arbitrariness in the determination of model parameters (especially the stiffness of the descending branch) poses a serious drawback in practical application of the model. Ref.7 reports divergence in dynamic analysis based on the trilinear model. It can be seen from **Fig.3** that when large displacement leads to significant drop in strength on one side, the nominal elastic range will expand on the other side (kinematic hardening). In such case, the more strength drops on one side, the stronger resistance for the overall displacement to return to neutral. Thus formulation of the trilinear model can contribute to divergence in dynamic analysis.

(3) Limiting application range of the trilinear model in view of its non-degrading nature is necessary. At least, the application range should be limited to $H_r \geq H_y$.

(4) Appropriate application range for D model is that the calculated damage index $D \leq 1.0$ (or horizontal strength of the structure $H_r \geq H_y$). Beyond this range, there is no guarantee that the analysis results have equal reliability.

(5) Although hard to quantify at present, extremely large displacement is prohibitive to the application of 2-para model.

(6) It can well be said that specifying an appropriate application range of a model is indispensable to its practical application; and check of application range can not be ignored in interpreting analysis results from any hysteretic models. This issue, however, has often been neglected in numerous developments of hysteretic models.

(7) Within an approriate application range (e.g. in terms of damage index $D \leq 1.0$), agreement between D model and 2-para model is quite satisfactory except for residual displacement under Type I · Ground Type III accelerograms. Actually, there is little common ground among the three models (D model, 2-para model and the trilinear model) when it comes to predicting residual displacement under Type I · Ground Type III accelerograms. Under other design accelerograms, the three models give very similar trend in predicted responses, but the residual displacement predicted by the trilinear model occasionally goes much higher than D model and 2-para model, which may be due to the non-degrading nature of the trilinear model.

(8) In terms of numerical stability, realistic hysteretic loops and comprehensiveness, D model is the most mature and well-developed model of the four hysteretic models examined in this study. Although it leaves out cyclic hardening effect in its formulation, D model errs

on the safe side in this regard.

(9) The extreme responses of bridge piers with short natural period to Level 2 · Type II accelerograms found in this study indicates that the priliminary design based on the seismic coefficient method may have much to be modified in the ultimate limit state design stage. Development of inelastic priliminary design method considering structural characteristics (such as natural period) shall be a great progress in design method, and makes a topic worth further research.

ACKNOWLEDGEMENTS: The authors want to thank the joint research group of Public Works Research Institute, Metropolitan Expressway Public Corporation, Hanshin Expressway Public Corporation, Nagoya Expressway Public Corporation, Kozai Club and Japan Association of Steel Bridge Construction for providing pseudodynamic test data used in this paper.

APPENDIX A

Major differences of hysteretic rules among the three sub-models (Type "A", Type "B", and Type "C") of the original 2 parameter model is summarized here:

(1) During the hardening stage, sub-model Type "B" accounts for cyclic hardening effect by stretching the nominal elastic range, while Type "A" and Type "C" do not (elastic range remains at H_y).

(2) Hysteretic rules during the degrading stage are identical for sub-model Type "B" and Type "C", they differ from those of Type "A" in two respects: one is that sub-model Type "B" and Type "C" always use the original skeleton curve while the skeleton curve is updated under certain conditions in Type "A"; the other is that the descending limb begins at δ_{max} in Type "A" (the maximum displacement ever reached), while in Type "B" and Type "C", it starts at the constant δ_m. It is recognized that these rules of Type "A" offers parameter $\bar{\beta}$ much larger space to adjust the rate of strength deterioration, and 2-para model has succeeded these features of sub-model Type "A" in its formulation.

APPENDIX B

Modeling of hysteretic behavior under one-sided cyclic loading demonstrates pointedly the effect of modifications made in the integrated 2 parameter model (2-para model) over the original 2 parameter model. **Fig.A1** is horizontal load — horizontal displacement curve ($H-\delta$ curve) generated by FEM analysis (details can be found in Ref.6) for a pipe-section steel bridge piers of $R_t = 0.075$, $\bar{\lambda} = 0.30$, $P/P_y = 0.15$. **Fig.A2** and **Fig.A3** are modeling of this hysteretic procedure by the original model (sub-model Type "A") and 2-para model respectively. The difference is clear at a glance: in **Fig.A2**, strength degradation begins on the positive load side once the displacement goes beyond δ_m, but on the negative side, strength degradation never is triggered since displacement can not reach $-\delta_m$ (Such severed judgement of beginning of strength degradation is common to all the three sub-models of the original 2 parameter model). This fault is corrected in 2-para model and it gives a much more realistic simulation in **Fig.A3**.

APPENDIX C

When it comes to modeling of hysteretic behavior under cyclic loading, D model and 2-para model give much more realistic simulation than trilinear or bilinear model which do not consider strength and stiffness degradation of pipe-section steel bridge piers. To illustrate this point, **Fig.A4** compares the simulation of the four models and the cyclic behavior predicted by FEM analysis (details can be found in Ref.6) of a pipe-section steel bridge piers of $R_t = 0.075$, $\bar{\lambda} = 0.35$, $P/P_y = 0.15$.

REFERENCES

1) Design Specifications of Highway Bridges (Part V. Seismic Design), Japan Road Association, December, 1996 (In Japanese).
2) Suzuki, M., Usami, T., Terada, M., Itoh, T. and Saizuka, K.: Hysteretic model and inelastic seismic analysis of box-section steel bridge piers, *J. Strut. Mech. and Earth. Engrg.*, JSCE, No.549/I-37, pp.191-204, October, 1996 (In Japanese).
3) Kumar, S. and Usami, T.: An evolutionary-degrading hysteretic model for thin-walled steel structures, *Engineering Structures*, Vol. 18, No.7, pp.504-514, 1996.
4) Kindaichi, T., Usami, T. and Kumar, S.: A hysteresis model based on damage index for steel bridge piers, *Journal of Structural Engineering*, JSCE, Vol. 44A, pp.667-678, March, 1998 (In Japanese).
5) Liu, Q.Y., Kasai, A. and Usami, T.: Parameter identification of damage-based hysteretic model for pipe-section steel bridge piers, *Journal of Structural Engineering*, JSCE, Vol.45A, pp.1005-1016, March, 1999.
6) Gao, S. B., Usami, T. and Ge, H. B.: Ductility evaluation of steel bridge piers with pipe sections, *Journal of Engineering Mechanics*, ASCE, Vol. 124, No.3, pp.260-267, 1998.

7) Joint Research Report on Limit State Seismic Design of Highway Bridge Piers (VII), Public Works Research Institute, Metropolitan Expressway Public Corporation, Hanshin Expressway Public Corporation, Nagoya Expressway Public Corporation, Kozai Club and Japan Association of Steel Bridge Construction, 1997 (in Japanese).

(Received January 7, 1999)

鋼製パイプ断面橋脚の復元力特性の比較

劉　青芸・葛西　昭・宇佐美　勉

本研究では，鋼製パイプ断面橋脚に対する４つの復元力モデル，すなわち：バイリニアモデル，トリリニアモデル，統合２パラメータモデルおよびダメージインデックスモデルによる弾塑性地震応答解析結果を比較することを目的としている．結果として，強度および剛性の劣化を考慮していないバイリニアモデルは，残留変位を精度良く予測できないことを示した．また，トリリニアモデルによる解析結果は，バイリニアモデルに比べて，統合２パラメータモデル，あるいはダメージインデックスモデルによる動的解析結果に近いが，繰り返しによる強度劣化および剛性劣化を考慮していないため，適用範囲などに注意する必要があることを示した．最後に，レベル２・タイプⅠ・Ⅲ種地盤地震動に対する残留変位を除いて，統合２パラメータモデルとダメージインデックスモデルを用いた解析結果が適用範囲 $H_r \geq H_y$ (H_r=終局強度)において良く一致していることを示した．